The Strain Rate Dependent Plastic Flow Behavior of Zirconium and its Alloys

D. LEE

The effect of strain rate ($10^{-5} \sim 10^{-1}$ min^{-1}) on the plastic flow behavior was examined by means of tension tests over a range of temperatures ($RT \sim 500°C$). The principal material examined was Zircaloy-2, and the others were iodide zirconium and binary alloys of Zr-0.1 pct O and Zr-1.5 pct Sn by weight. In Zircaloy-2, the behavior was characterized by a sudden increase of flow strength with decreasing strain rate; concurrently the ductility decreased. Other interrupted and hold time experiments showed that the process is essentially that of a strain rate-induced strengthening phenomenon, with several features which could be identified with the strain aging process. It was further shown that the critical range of strain rates and temperatures at which the anomalous behavior took place could be correlated with the minimum in the strain rate sensitivity of flow stress. A similar but less pronounced flow behavior was observed with pure zirconium and its binary alloys, but with no marked change in the tensile ductility. From these results, the role of oxygen and tin on the early stage of plastic flow behavior was discussed in terms of dislocation-impurity interaction mechanisms. It was however concluded that these elements are not directly responsible for the ductility loss at slow strain rate in Zircaloy-2.

IN recent years it has become increasingly evident that zirconium and some of its alloys exhibit an anomalous mechanical behavior over the temperature range of approximately 200° to 400°C. The observed phenomena in this temperature range include the yield-point effect and the flow stress increase after interrupted loading in tension testing,[1-10] the decreasing creep rate with increasing temperature,[11-13] and the decreasing tensile ductility with both increasing temperature[12,14] and decreasing strain rate.[15] Many of these phenomena have been related to some form of strain aging, and a variety of mechanisms have been proposed. For example, the effects have been associated with the precipitation of tin in Zr-1.5 Sn alloy,[2] with hydrogen segregation in Zircaloy-2,[5] with the Cottrell locking of dislocations by impurity atmosphere,[13] or with the other dislocation-interstitial interactions, such as with oxygen.[8,9] The dynamic dislocation model for yielding also has been applied to explain the yield-point behavior.[6]

Other related anomalies in these alloys have also been reported. It was found that the apparent activation energy in creep increased abruptly followed by a sharp drop at about 350°C.[13,16] This was again attributed to a solute-dislocation interaction. Another notable characteristic is that of the sharply lower strain rate sensitivity of the flow stress in the temperature range of 300° to 400°C in pure zirconium,[7] Zircaloy-2,[3] and Zircaloy-4.[17] Similar minima in strain rate sensitivity were also observed in single crystals both of Zircaloy-2[18,19] and zirconium oxygen alloys.[20,21]

For some of the widely used complex commercial alloys like Zircaloy-2, this anomalous behavior has not yet been adequately characterized. The multiplicity of alloying elements in addition to tin and oxygen in such alloys is the reason for this lack of understanding. It is therefore important that the nature of this anomalous behavior be identified and also that the flow-stress behavior up to and including fracture be characterized.

An attempt was made in this work to establish the phenomenology of the stress-strain rate-temperature relationship in Zircaloy-2 as well as the strain-rate dependence of the fracture strain. Also examined were the effects of alloying elements such as oxygen and tin in zirconium in amounts comparable to those found in Zircaloy-2. The mechanical behavior of these alloys were in turn compared with that of pure zirconium, where the structure and testing conditions were comparable.

EXPERIMENTAL PROCEDURE

Processing and Structures

Both iodide grade zirconium and Zircaloy-2 were obtained in the form of forged ingots. The binary alloys of oxygen and tin were prepared by remelting the same iodide grade zirconium using a vacuum arc melting method. The details of the subsequent thermal-mechanical processing schedule are given in Table I; the final recrystallization treatment was designed to produce comparable grain sizes in all the materials. The microstructures of the recrystallized materials are shown in Fig. 1. The results of the chemical analyses made after the final heat treatment are shown in Table II.

The crystallographic texture was determined by the Siemens' pole-figure device, described elsewhere.[15] The pole figure of Zircaloy-2 was nearly the same as that of Schedule J in the previous work,[15] *i.e.*, the (0002) pole was tilted about 35 deg from the sheet normal toward the transverse direction. A similar texture was found for the iodide grade zirconium. The texture of the binary alloy sheets was not determined since the measurements of the transverse strain in

D. LEE is Metallurgist, General Electric Research & Development Center, Schenectady, N. Y.

Manuscript submitted September 30, 1969.

tension indicated a behavior similar to the pure zirconium.

Tensile Specimens and Testing

The orientation of all specimens was such that the specimen axis was parallel to the transverse direction in the sheet. The gage section was 0.2 by 0.055 in. and 0.8 in. long. A strain extensometer was used over a 0.5 in. portion of the gage length in all the tests.

All tests were conducted in an Instron machine. At elevated temperatures, tests were made in an Instron chamber containing a helium atmosphere. Three types of tests were used: monotonic straining to fracture at a fixed crosshead speed, interrupted straining where prestrain, hold time, and crosshead speed were varied, and finally, differential strain rate tests. In the latter tests, the crosshead speed was varied from 2×10^{-5} in. per min to 2 in. per min in a manner shown schematically in Fig. 2. Since the material always strain hardens, the load extrapolation method shown in Fig. 2 was used in the differential strain rate tests to obtain a

Table I. Processing History and Material Details

Material	Initial Condition	Primary and Final Working	Final Treatment	Grain Size, μ
Iodide grade Zr	3/4 in. thick plate cut from a forged ingot	Hot roll to 0.140 in. in thickness at 400°C and rolled at *RT* to 0 062 in.	600°C/25 min	9.5
Zr + 0.1 pct O	Vacuum arc melted and machined disc of 0.320 in. in thickness	Upset at 930°C to 0.220 in. in thickness and rolled from 400°C to 0.062 in.	640°C/1½ hr	9.4
Zr + 1.5 pct Sn	Vacuum arc melted and machined disc of 0.320 in. in thickness	Upset at 930°C to 0.220 in. in thickness and rolled from 400°C to 0.062 in.	640°C/1½ hr	8.5
Zircaloy-2	1 in. thick plate cut from a forged ingot	Hot roll from 900°C to 0.160 in. in thickness followd by cold rolling to 0.062 in. in thickness	750°C/45 min	11.0

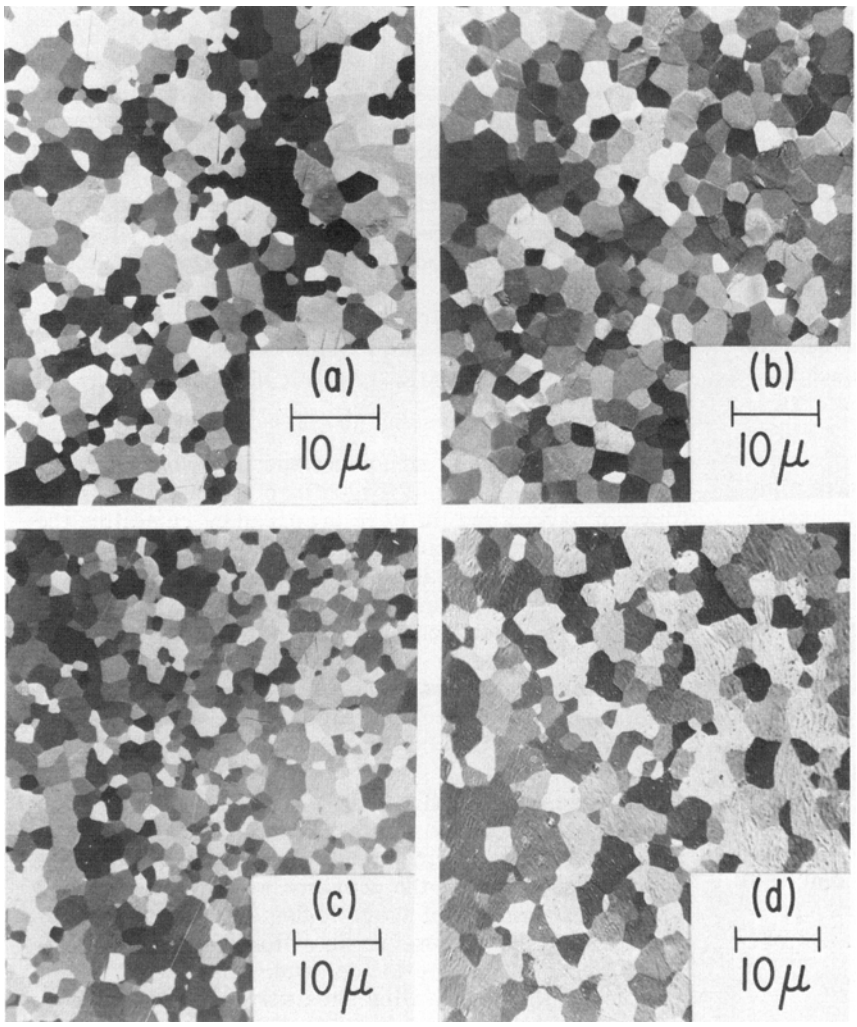

Fig. 1—Representative microstructures as in the recrystallized condition: (*a*) Iodide grade zirconium, (*b*) Zr-O alloy, (*c*) Zr-Sn alloy, and (*d*) Zircaloy-2. Prior to the final mechanical polish the specimens were etched in a solution of 2.5 parts HF, 22 parts HNO_3, and 45 parts lactic acid with 22 parts water. Rolling direction is vertical.

Table II. Composition of the Alloys

ppm by weight, except otherwise specified

Material	Sn	Fe	Cr	Ni	O	N	H	C	Al	Cu	Ta	Cd	Hf
Iodide grade Zr	<10	400	<10	<10	86	25	5	50	300	<10	<100	<10	200
Zr + 0.1 pct O	<10	300	<10	<10	1330	22	38	20	200	20	<100	<10	200
Zr + 1.5 pct Sn	1.47, pct	300	<10	<10	68	12	37	55	300	500	<100	<10	200
Zircaloy-2	1.51, pct	1380	900	500	1035	32	38	110	50	10	<100	<10	<100

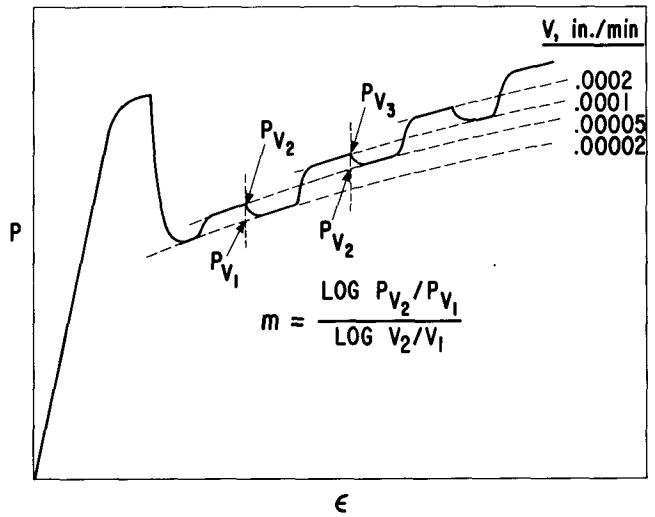

Fig. 2—A schematic diagram showing how the strain-rate sensitivity of flow stress, m, was obtained from the load, P, vs extension, ϵ, curve in the differential strain-rate test. The load extrapolation method is also indicated.

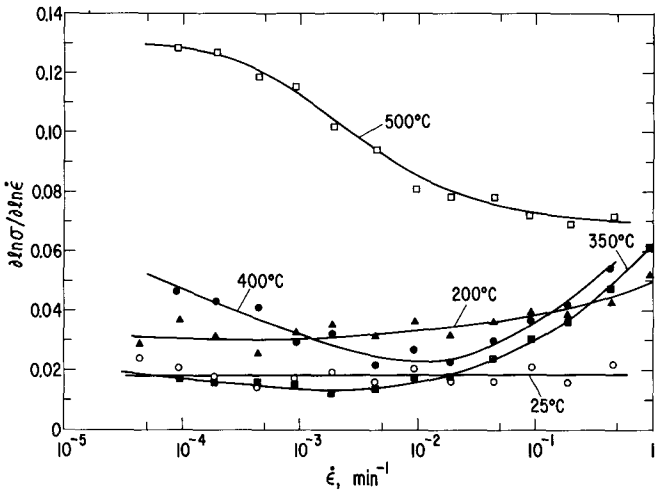

Fig. 3—The strain-rate dependence of the strain-rate sensitivity of flow stress, $m(\dot{\epsilon}) = (\partial \ln \sigma/\partial \ln \dot{\epsilon})$, for Zircaloy-2 at selected temperatures.

measure of strain rate sensitivity of flow stress, $m = \partial \ln \sigma/\partial \ln \dot{\epsilon}$ where σ is the flow stress and $\dot{\epsilon}$ the strain rate.

Electron Metallography

Specimens for electron transmission microscopy were first ground to about 0.005 in. in thickness, then electrolytically thinned in a solution of 950 ml acetic acid and 50 ml perchloric acid.

RESULTS

Phenomenology in Zircaloy-2

The increased flow stress in subsequent reloading after a load interruption is evidence that this alloy exhibits strain aging characteristics. Since such an interrupted loading method however involves a large number of test variables, alternative methods were used to broadly characterize the mechanical behavior of Zircaloy-2. These include the differential strain-rate technique and monotonic tension testing.

The results of the differential strain rate tests are shown in Fig. 3 where the calculated m values are plotted over the range of strain rates. The overall level of m is lower at 350°C than at other test temperatures for most of the strain rates examined. At all temperatures except 400° and 500°C, the values of m tend to increase with increasing strain rate. Cross-plotting Fig. 3 at selected strain rates yields the temperature dependence of m as shown in Fig. 4. The

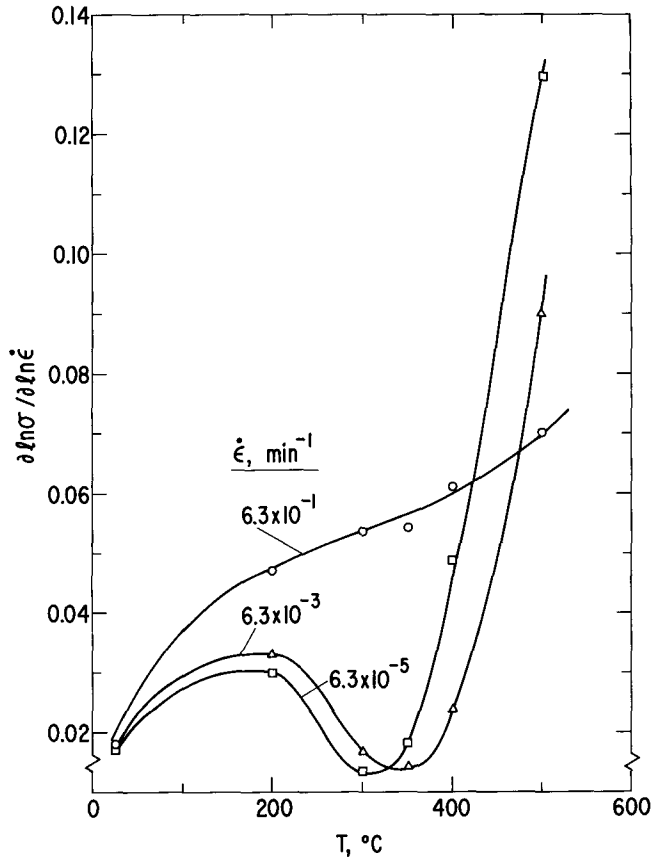

Fig. 4—The temperature dependence of the strain-rate sensitivity of flow stress, m, in Zircaloy-2 from room temperature upwards at selected strain rates.

value of m does not increase monotonically with temperature as is the case for a simple thermally activated process, but is substantially depressed over a broad temperature range, reaching a minimum over the temperature range of ~300° to 350°C. Above this temperature range, m increased sharply. This may be an indication that with further increase in temperature m will increase to a very large value as in the case of superplastic Zircaloy-4.[17]

Monotonic tensile tests were carried out to strain at fracture at various strain rates at 350°C, the temperature that corresponds to the minimum value of m in Fig. 4. In the region of uniform strain, the effect of changes in strain rate on the flow stress confirm the expectations from the m measurement, as shown in Fig. 5. As the strain rate decreased below 6.3×10^{-3} min^{-1}, the flow stress at a fixed strain increased, Fig. 6; the strain rate sensitivity of flow stress is therefore negative, as has been observed in other alloys.[22,23] The flow stress depends on strain in a peculiar manner, as shown by the true stress-true plastic strain relationship of Fig. 7. Except at the fastest strain rate ($\dot{\epsilon} = 6.3 \times 10^{-1}$ min^{-1}), the data at each rate could be approximated by two sets of straight lines. As shown in Table III the strain hardening exponent also decreased with increasing strain.

Another characteristic behavior of these materials is the substantially reduced fracture elongation at slow strain rates as seen in both Figs. 5 and 8. This is consistent with previous observations.[15] The pertinent tensile data are summarized in Table III. With decreasing strain rate the uniform strain decreased more than a factor of 2; the necking strain was reduced but the reduction of area was not appreciably altered. The details of the fracture process and its strain rate dependence will be described in a separate paper.[24]

Further insight into the process leading to these anomalous stress-strain relationships can be gained from a series of controlled interrupted loading tests. A total of four such tests were made, the loading schedules and results being presented in Fig. 9. The results are represented by the solid lines and compared with the reference test data at two strain rates which are indicated by dotted lines in all four cases. In the first test (A), the specimen tested at the fast strain rate was given the same thermal history as that tested at the slow strain rate by preheating the specimen at the testing temperature for an appropriate time before testing. This preheating had essentially no effect. In the second test (B), the effect of prestrain and aging under stress was examined. The specimen was given an initial 5 pct deformation at the fast strain rate; the load was then maintained at temperature for a time comparable to that of slow strain rate test. When it was pulled again at the fast strain rate, the specimen fractured at a strain comparable to that of the uninterrupted fast strain rate test. In the third test (C), the specimen was tested at the fast strain rate after a 5 pct prestrain at the slow strain rate. The fracture strain was again similar to that obtained from the fast strain rate test. Tests (B and C) show that the strain to fracture at fast rate is not path dependent if the load is interrupted before it reaches the maximum load. The final interrupted test (D) was approximately the converse of test (C); the specimen

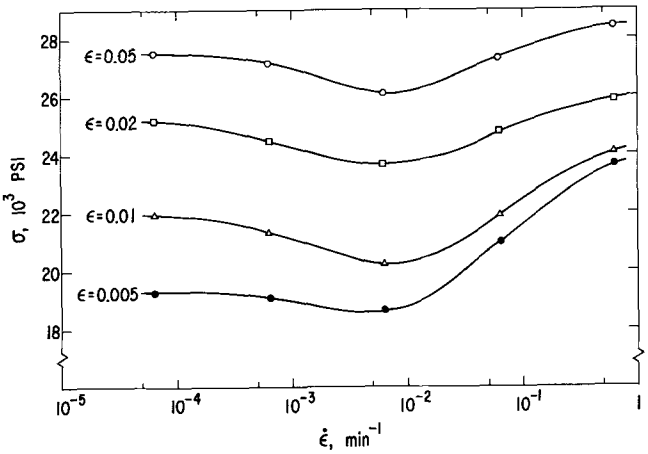

Fig. 6—Engineering stress, σ, vs strain rate, $\dot{\epsilon}$, curves for Zircaloy-2 tested at 350°C and at various levels of engineering strain.

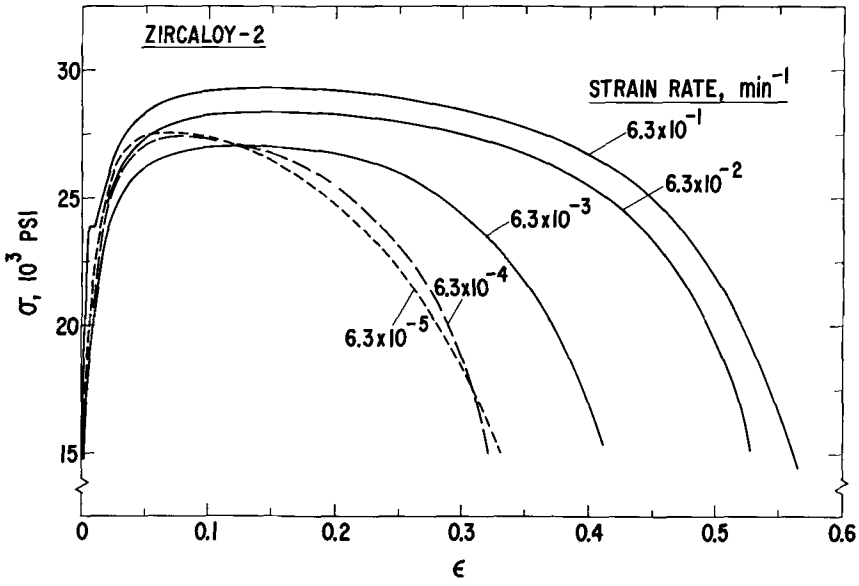

Fig. 5—Engineering stress, σ, vs engineering strain, ϵ, curves for Zircaloy-2 tested at 350°C and at various initial strain rates.

was tested at the slow strain rate after a 10 pct pre-strain at the fast rate. The resulting fracture strain was comparable to that obtained when the entire test was conducted at the slow strain-rate test. From these tests it can be inferred that tensile ductility is strongly dependent on the strain rate prevailing during the fracture process.

Effect of Alloying Elements

The effect of two important alloying elements on the mechanical behavior of zirconium was examined by testing each alloy at two strain rates sufficiently different that the changes in the flow stress and ductility would be large enough to be easily compared. The complete stress-strain curves are given in Fig. 10 and the data are included in Fig. 8 and Table III. The ductility decrease at low strain rates observed in Zircaloy-2 is absent in all the other materials. On the other hand, some anomalies in the flow stress behavior are also observed in these materials; the flow stress at two strain rates cross over with increasing strain in Zr-Sn alloy but they show little difference at small strain in both iodide Zr and Zr-O alloy. A selected differential strain rate test with iodide Zr indicated m also approaching zero at 350°C.

For all the materials including Zircaloy-2 the uniform strain decreased with decreasing strain rate, Table III. The principal difference between Zircaloy-2 and the rest of the metals is that the necking strain decreased with decreasing strain rate in Zircaloy-2 while the reverse was true for all the other materials tested. Finally, for all the materials except Zircaloy-2 the strain hardening exponent decreased with decreasing strain rate.

Internal Structure

If precipitates form preferentially around dislocations or grain boundaries or if dislocations cluster

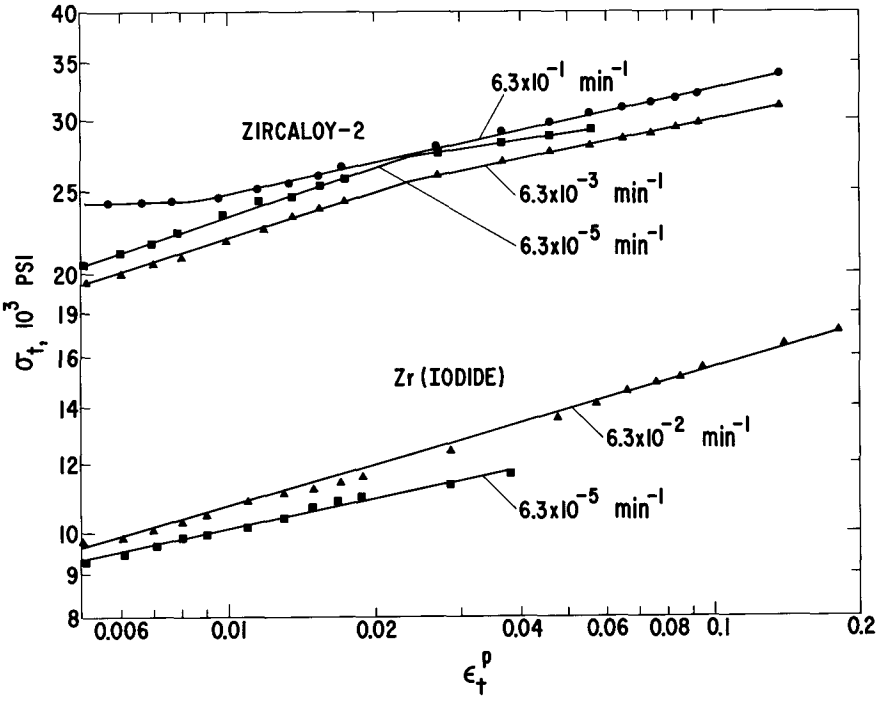

Fig. 7—True stress, σ_t, vs true plastic strain, ϵ_t^p, relationships for Zircaloy-2 and iodide zirconium tested at 350°C and at various strain rates.

Table III. Additional Tensile Data

Material	Strain Rate, min^{-1}	Uniform Strain ϵ_u, pct	Necking Strain ϵ_n, pct	Total Elong. EL, pct	Reduction of Area RA, pct	Strain Hard. Exponent, n
Iodide grade Zr	6.3×10^{-2}	15	39	54	92	0.18
	6.3×10^{-5}	4	79	83	95	0.12
Zr + 0.1 pct O	6.3×10^{-2}	25	25	50	85	0.20
	6.3×10^{-5}	15	53	68	88	0.16 (ϵ<0.024) 0.09
Zr + 1.5 pct Sn	6.3×10^{-2}	27	25.5	52.5	87.5	0.19
	6.3×10^{-5}	20.5	34.5	55	74.5	0.16
Zircaloy-2	6.3×10^{-1}	16	40	56	81	0.12
	6.3×10^{-2}	15.5	37.5	53	81	0.13
	6.3×10^{-3}	14	28	42	79	0.18 (ϵ<0.025) 0.12
	6.3×10^{-4}	8	24	32	77	0.18 (ϵ<0.026) 0.10
	6.3×10^{-5}	6.5	26.5	33	77	0.19 (ϵ<0.025) 0.08

around impurities during the deformation, they would be directly identifiable by transmission electron microscopy.

A preliminary examination was made on specimens which were heated to 350°C only without any plastic deformation. The structure was not distinctive except for the presence of about 0.2 μ particles in Zircaloy-2. To facilitate the interaction of impurities with dislocations both iodide zirconium and Zircaloy-2 were strained 5 pct total strain at room temperature followed by aging at 350°C for $\frac{1}{2}$ hr. The resulting structures, shown in Fig. 11, again show no distinctive features. An early stage of hydride platelet development from the thinning procedure is seen in the iodide zirconium [Fig. 11(*a*), lower right hand corner]. In Zircaloy-2, the dislocations are more or less random, except for minor evidence of clustering at a few areas.

The structures of the specimens actually deformed at 350°C were compared with these reference structures, Fig. 12. While no special features can be seen in the iodide zirconium, the clustering of dislocations around impurities can be observed in Zircaloy-2 as the tensile strain increases [Figs. 12(*b*) and 12(*c*)]. The clustering network in Fig. 12(*c*) was identified as consisting of dislocations by tilting the stage during the observation. The exact nature of this clustering is unknown however.

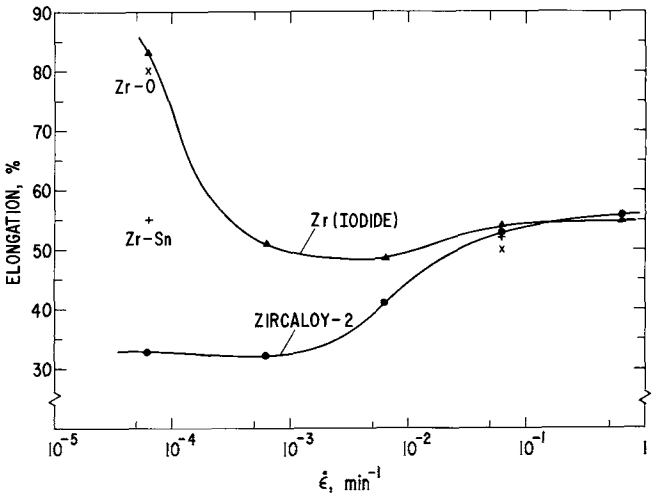

Fig. 8—Total tensile elongation vs initial strain rate, $\dot{\epsilon}$, for various materials tested at 350°C. For both Zr-O and Zr-Sn binary alloys, tests were made only for two strain rates.

DISCUSSION

The most readily observable deviation in the behavior of zirconium and some of its alloys from the generally observed phenomenological relationship between stress, strain rate, and temperature is the strain rate dependence of the flow stress over the temperature range of 200° to 350°C. The decreasing m with increasing temperature as seen in the differential strain-rate tests with Zircaloy-2 is consistent with the behavior in the monotonic tension testing over the same temperature range and with the sharply increasing activation energy.[13,16] Attempts have been made to relate such behavior with the changes in other deformation parameters, such as activation volume.[20,21] Alternatively, a decreasing m could be identified with an increasing stress-dependent dislocation density and velocity. No specific conclusion can be derived from such relationships, however.

On the other hand, a large value of m, as great as ~0.8,[17,25] has been shown to be a necessary condition for superplastic behavior.[26,27] That rationale for superplasticity however cannot be applied to the case of m approaching zero as it has been done elsewhere,[28] since all it implies is that there will be little contribution to steady flow from strain-rate hardening. Instead, other parameters such as strain hardening and processes leading to fracture can influence more directly the magnitude of tensile ductility.

It has been suggested, however, that a reduced strain-rate sensitivity of the flow stress is associated with strain-aging behavior, as demonstrated by Lubahn[29] and Pugh.[30-32] A similar behavior has also been observed for commercially pure titanium.[22,33,34] Consequently, m values can be usefully applied to identify the regions of temperature and strain rate where the flow behavior has an anomalous characteristic.

Other flow characteristics have also been attributed

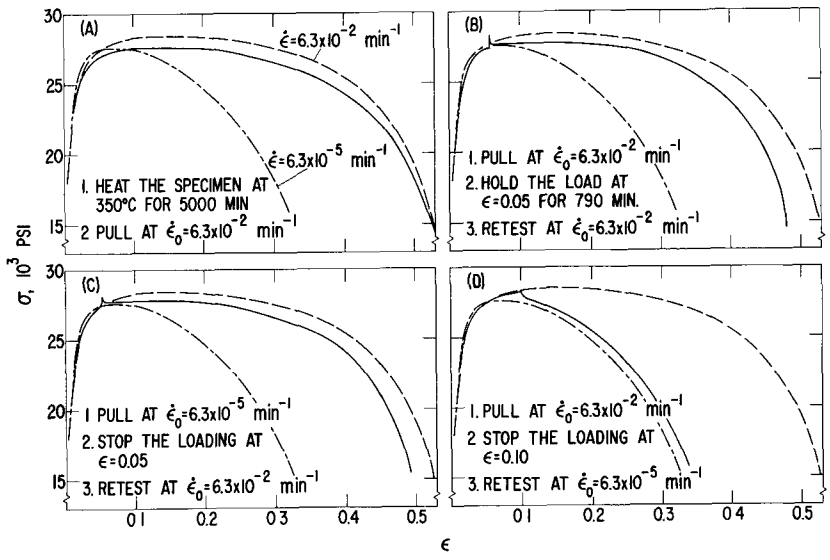

Fig. 9—The results of various load interruption tests made with Zircaloy-2 at 350°C. The detailed procedure for schedules (A) through (D) is indicated in each figure as well as the result by the solid lines.

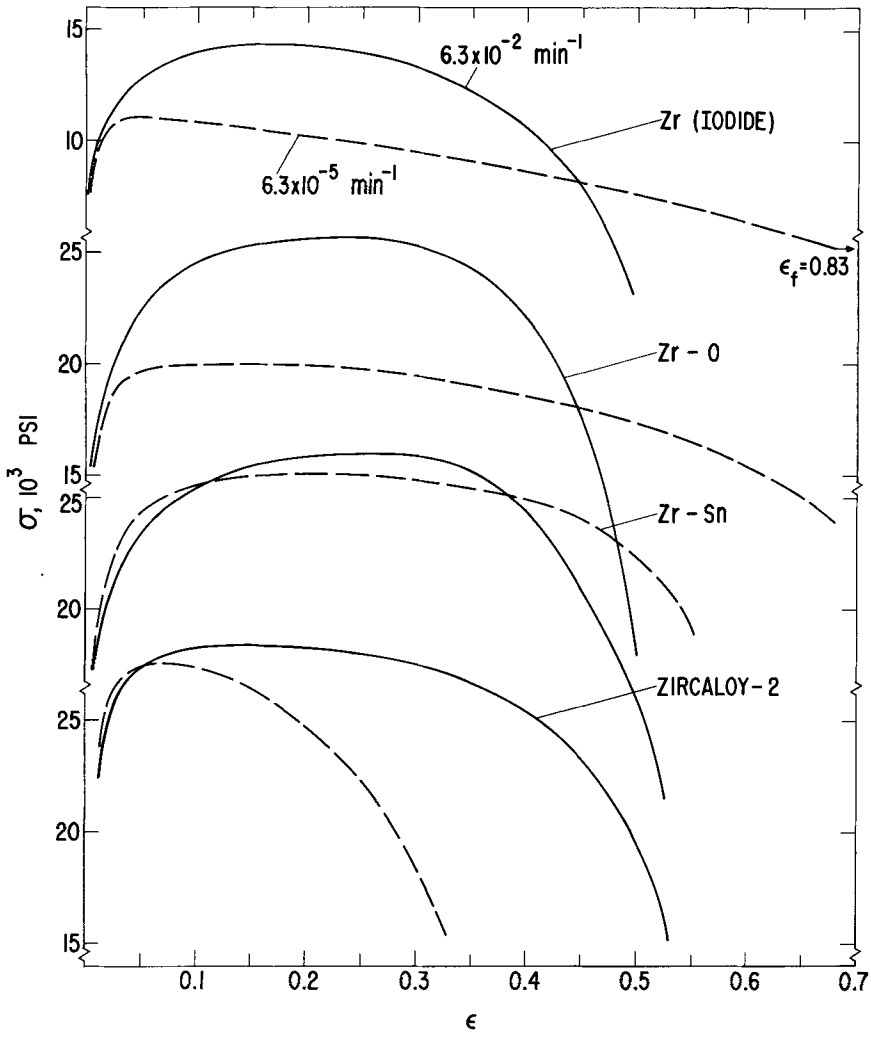

Fig. 10—Engineering stress, σ, vs engineering strain, ϵ, curves for all the materials tested at 350°C and at two initial strain rates.

to a strain-aging phenomenon; among them are increasing flow strength with temperature, discontinuous plastic flow, and yield-point phenomena. In Zircaloy-2, however, neither a marked increase in flow stress nor discontinuous flow accompanied the low value of m observed. A yield-point effect, however, has been observed in zirconium and its alloys at finer grain size or increased test temperatures.[5,6,10] Therefore, if the behavior of zirconium could be described as strain aging, it is by no means as pronounced as in mild steel. The result of internal friction experiments also indicated that the peak was poorly defined[4] and thus the mechanism could not be clearly identified.

Some aspects of the phenomenology has been established by the load interruption testing of Zircaloy-2. The strain rate prevailing at the completion of the test was shown to affect the necking strain, independent of the prior rate history. The tensile ductility may be path dependent only to the extent that both uniform and necking strains are separately dependent on the strain rate. With iodide Zr, Zr-O, and Zr-Sn alloys the necking strain increased with decreasing strain rate in contrast to the result with Zircaloy-2. One possible inference is that the mechanisms controlling the flow processes are different for the two regions of strain.

If the phenomena observed in Zircaloy-2 are a direct consequence of some form of dynamic instability,[35] such as causes the blue brittleness of steel or the Portevin-Le Chatelier effect, the strain hardening coefficient, $n = (\partial \ln \sigma / \partial \ln \epsilon)$, should increase with decreasing strain rate. An indication of this was observed in Zircaloy-2, but the reverse trend was seen in the other materials. Moreover, the decreasing n with increasing strain as seen in Zircaloy-2 and Zr-O alloy is an indication of the change in the deformation mechanism with strain, the change in hardening presumably resulting from a dislocation-impurity interaction. Dislocations will be stopped in the hardening process and pinned by impurities until they become free again from the impurity clouds. If the phenomenon is the result of such an impurity-dislocation interaction, the effects of temperature and strain rate can be in principle estimated.

Fridel[35] has shown for example that the maximum temperature for the appearance of dynamic instability effects is governed by two conditions. One is that the impurity clouds must saturate the dislocations. Therefore, the concentration of impurity and temperature can be related to the interaction energy for impurity and dislocations.[36] Since, however, the value for the interaction energy is unknown, they could not be readily estimated. Secondly, the impurity clouds must not diffuse too quickly and the strain rate must be sufficiently large that the dragging of unsaturated impurity clouds does not occur. This rate is given by the

equation, $\dot{\epsilon} > (2\rho D\sigma b^3/kT)$, where ρ is the mobile dislocation density, D the diffusion coefficient of impurity, and σ the applied stress. Substituting values for those quantities that can be estimated, such as $\rho = 10^9$ per sq cm, $\sigma = 28{,}000$ psi (19.3×10^8 dynes per sq cm), $T = 623°K$ and $b^3 = 15 \times 10^{-24}$ cm^3, it yields the following relation:

$$\dot{\epsilon} > (6.75 \times 10^8) D \ (1/\text{sec})$$

If a value of the diffusion coefficient of oxygen, the principal interstitial element, equals to 2.2×10^{-17} sq cm per sec at 350°C is selected from the presently controversial range of diffusion coefficients available,[37,38] the equivalent strain rate is about 10^{-6} min^{-1}. This is within about two orders of magnitude of the strain rate at which the pronounced effect was observed. No specific interaction process can be identified, but this does point out the possible contribution of a dislocation-interstitial interaction in contrast to an earlier suggestion that such an interaction mechanism does not exist.[36]

Certainly no specific element has been established as responsible for the unusual stress-strain rate relationship in zirconium alloys other than to recognize the possible contribution of oxygen which has also been shown to produce the athermal component of stress.[19,20] Tin also cannot be ruled out because it gave rise to a similar trend in the early stage of deformation. Furthermore, a possible contribution of carbon should be recognized because all the materials contained carbon over the range of about 50 to 100 ppm. Moreover, carbon has one of the lowest solubility in zirconium and therefore it may have the largest interaction energy of the alloying elements. This would imply that dislocations may tend to cluster more around carbon atoms.

Zircaloy-2 is obviously too complex to identify any specific impurity effect. In addition to the interstitial elements discussed, it may contain several intermetal-

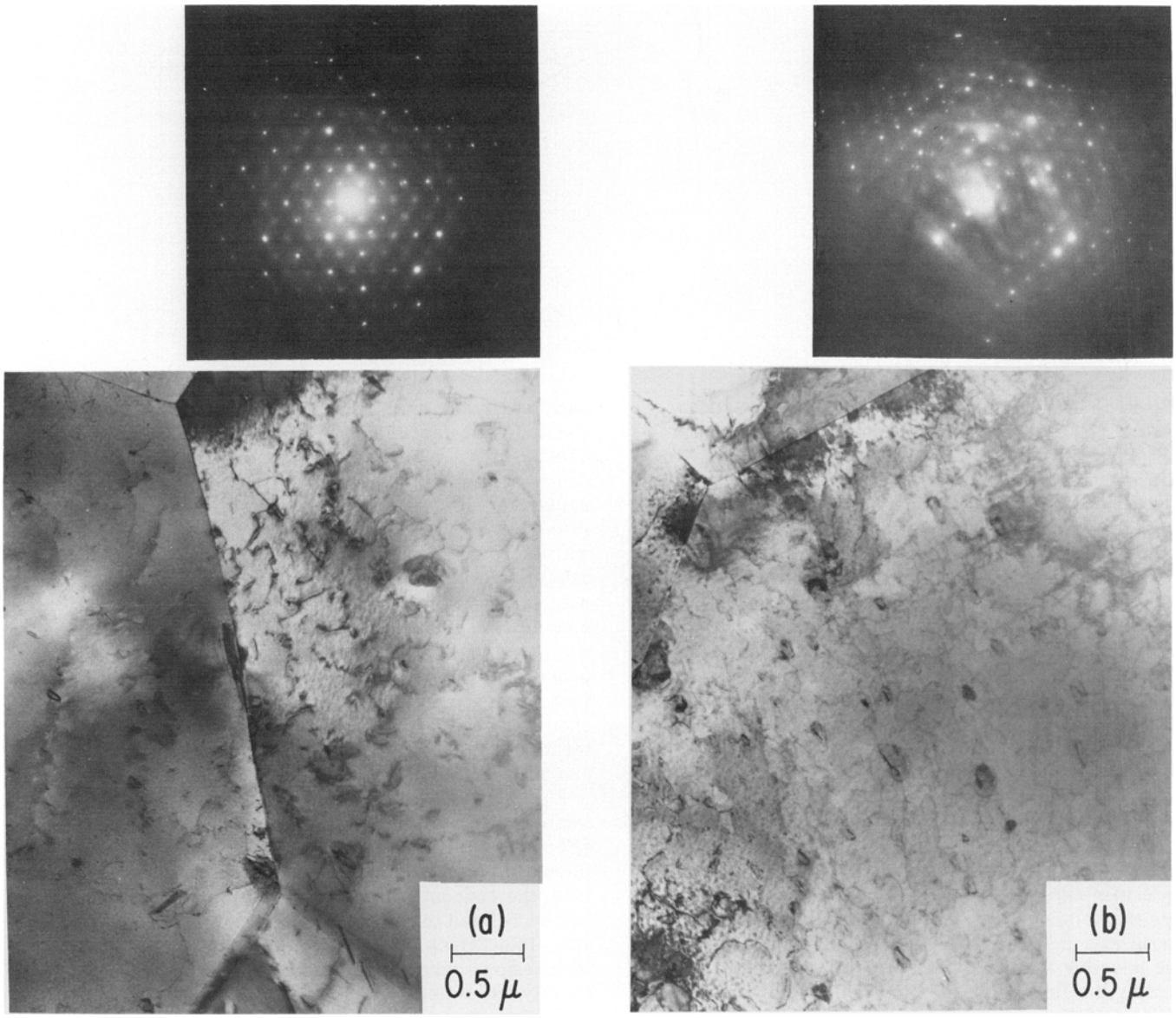

Fig. 11—Structures of (*a*) iodide zirconium and (*b*) Zircaloy-2 deformed at room temperature to 5 pct in strain and heated to 350°C for 1 hr. The diffraction patterns are also included.

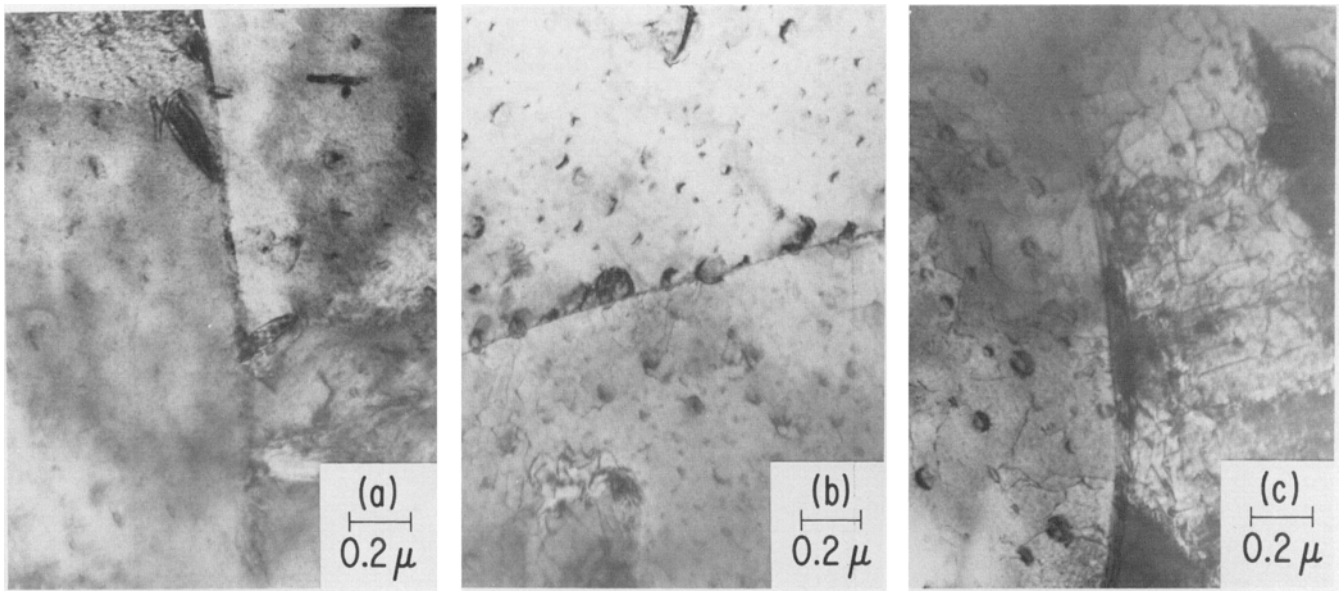

Fig. 12—Structures in the deformed condition at 350°C: (*a*) iodide zirconium deformed to 5 pct in strain; (*b*) Zircaloy-2 deformed to 5 pct in strain; (*c*) Zircaloy-2 deformed to fracture, 33 pct, but examined in the area corresponding to the uniform gage section. All the tests were made at the initial strain rate of $\dot{\epsilon} = 6.3 \times 10^{-5}$ min^{-1}.

lic compounds such as $ZrCr_2$, $ZrFe_2$, Zr_2Ni, and Zr_4Sn, at least in the binary form.[39] In fact it has been suggested that the strain induced precipitation of Zr_4Sn was responsible for the strain-aging behavior; this was used as a means of establishing the zirconium-rich end of Zr-Sn phase diagram.[40] Since the necking strain decreased with decreasing strain rate in Zircaloy-2 only, the strain-enhanced precipitation of a second phase in this alloy might be responsible. Indeed, Östberg[41] reported a second phase in Zircaloy-2 consisting largely of Fe, Ni, and Sn with Zr. The possibility of an additional strain-rate dependent deformation mechanism due to the formation of second-phase particles in the highly strained neck cannot be ruled out, since dislocation clustering was observed to be more distinct at higher strains.

CONCLUSIONS

1) Zircaloy-2 exhibits an anomalous stress-strain rate relationship near 350°C at the slow strain rate, $<6.3 \times 10^{-3}$ min^{-1}, by the flow stress increasing with decreasing strain rate. This is accompanied by a decreasing tensile ductility. The strain rate sensitivity of the flow stress, $\partial \ln \sigma / \partial \ln \epsilon$, also reaches a minimum at this region of temperature.

2) Several effects of alloying elements in pure zirconium have been identified. The addition of tin gives rise to a stress-strain rate behavior similar to that observed in Zircaloy-2, whereas the Zr-O alloy showed little strain rate effect in the very early stage of plastic deformation. The main difference between these alloys and Zircaloy-2 is found in the tensile ductility, since in contrast to Zircaloy-2 the necking strain in iodide zirconium, Zr-O, and Zr-Sn alloys increases with decreasing strain rate.

3) The ductility change in Zircaloy-2 with strain rate was shown to be strongly dependent on the prevailing strain rate. It is suggested that strain enhanced precipitation of a second phase consisting of Fe, Ni, and Sn with Zr may contribute to the reduced necking strain.

ACKNOWLEDGMENTS

The author is indebted to the members of the Metals Processing Unit for the alloy preparation and processing, P. T. Hill for tension testing, E. F. Koch for electron transmission microscopy, and C. R. Rodd for the metallography work. He is also grateful to L. F. Coffin and W. G. Johnston for useful discussions and H. C. Rogers for his critical comments.

REFERENCES

1. J. H. Keeler: *Trans. ASM*, 1955, vol. 47, p. 157.
2. L. Bangert: *Z. Metallk.*, 1959, vol. 50, p. 269.
3. R. L. Mehan and F. W. Wiesinger: KAPL Report 2110, 1961, KAPL, Schenectady, N.Y.
4. F. R. Shober, M. F. Getz, P. B. Shumaker, A. D. Young, M. F. Amateau, and R. F. Dickerson: Battelle Memorial Institute Report 1616, 1963, B.M.I., Columbus, Ohio.
5. G. Östberg: *J. Inst. Metals*, 1965, vol. 93, p. 223.
6. D. Weinstein: *Electrochem. Tech.*, 1966, vol 4, p. 307.
7. B. Ramaswami and G. B Craig: *Trans Met. Soc. AIME*, 1967, vol. 239, p. 1226.
8. K. Veevers and W. B. Rotsey: *J. Nucl. Mat.*, 1968, vol. 27, p. 108.
9. K. Veevers, W. B. Rotsey, and K. U. Snowden: Applications Related Phenomena in Zirconium and It Alloys, ASTM Spec. Tech. Publ., 458, p. 194 ASTM, Philadelphia, Pa., 1969.
10. D. V. Edmonds and C. J. Beevers: *J. Nucl. Mat.*, 1968, vol. 28, p. 345.
11. P. J. Pankaskie Hanford Report, HW-75267, 1962, G. E. Hanford Lab, Richland, Wash.
12. L. G. Bell: *Canad. Metal. Quart.*, 1963, vol. 2, p. 119.
13. V. Fidleris: Applications Related Phenomena in Zirconium and Its Alloys, ASTM Spec. Tech. Publ., 458, p. 1, ASTM, Philadelphia, Pa., 1969.
14. L. S. Rubenstein, J. G. Goodwin and F. L. Shubert: *Trans. ASM*, 1961, vol. 54, p. 20.
15. D. Lee: *Trans. ASM*, 1968, vol. 61, p. 742.
16. J. J. Holmes: *J. Nucl. Mat.*, 1964, vol. 13, p. 137.
17. D. Lee and W A. Backofen: *Trans Met. Soc. AIME*, 1967, vol. 239, p. 1034.
18. W. R. Tyson: *J. Nucl. Mat.*, 1967, vol. 24, p. 101.
19. W. R. Tyson: *Canad. Met. Quart.*, 1967, vol. 6, p. 301.
20. P. Soo and G. T. Higgins: *Acta Met.*, 1968, vol. 16, p. 177.
21. D. Mills and G. B. Craig: *Trans. TMS-AIME*, 1968, vol. 242, p. 1881
22. S. N. Monteiro, A. T. Santhanam, and R. E. Reed-Hill Proc. Intl. Conf. on

Titanium, London, England, May, 1968.
23. A. Nadai and M. J. Manjoine: *Trans. ASME*, 1941, vol. 63, p. A77.
24. D. Lee, E. Koch, and H. C. Rogers: G. E. Research & Development Center Report 70-C-075, 1969, G.E. R & DC, Schenectady, N.Y.
25. D. Lee: *Acta Met.*, 1969, vol. 17, p. 1057.
26. W. A. Backofen, I.R. Turner, and D. H. Avery: *Trans. ASM*, 1964, vol. 57, p. 980.
27. E. W. Hart: *Acta Met.*, 1967, vol. 15, p. 351.
28. D. A. Woodford: *Trans. ASM*, 1969, vol. 62, p. 291.
29. J. D. Lubahn: *Trans. ASM*, 1952, vol. 44, p. 643.
30. J. W. Pugh: *Trans. ASM*, 1955, vol. 47, p. 984.
31. J. W. Pugh: *Trans. ASM*, 1956, vol. 48, p. 677.
32. J. W. Pugh: *Trans. ASME*, 1957, vol. 209, p. 1243.
33. F. D. Rosi and F. C. Perkins: *Trans. ASM*, 1953, vol. 45, p. 972.
34. R. N. Orava, G. Stone, and H. Conrad: *Trans. ASM*, 1966, vol. 59, p. 171.
35. J. Friedel: *Dislocations*, Pergamon Press, p. 412, 1964.
36. G. R. Piercy. *J. Nucl. Mat.*, 1968, vol. 26, p. 18.
37. J. P. Pemsler: *J. Electrochem. Soc.*, 1964, vol. 111, p. 1221.
38. G. V. Kidson: *Electrochem. Tech.*, 1966, vol. 4, p. 193.
39. M. Hansen. *Constitution of Binary Alloys*, pp. 573, 741, 1062, 1219, McGraw-Hill, 1958.
40. G. R. Speich and S. A. Kulin. *Zirconium and Zirconium Alloys*, p. 197, ASM, Cleveland, 1953.
41 G. Ostberg: *J. Nucl. Mat.*, 1962, vol. 7, p. 103.